Intrinsic quantum melting of a driven vortex lattice in amorphous Mo_xGe_{1-x} films

S. Okuma and H. Imaizumi
Research Center for Low Temperature Physics, Tokyo Institute of Technology, 2-12-1, Ohokayama, Meguro-ku, Tokyo 152-8551, Japan

N. Kokubo
Center for Research and Advancement in Higher Education, Kyushu University, 4-2-1, Ropponmatsu, Chuoh-ku, Fukuoka 810-0044, Japan

(Received 22 September 2009; published 22 October 2009)

We observe melting of a driven vortex lattice in amorphous Mo_xGe_{1-x} films down to near-zero temperature using a mode-locking technique. We determine the dynamic melting line $B^{\infty}_{c,dyn}(T)$ in nearly the whole field-temperature (B-T) phase diagram. At low T, $B^{\infty}_{c,dyn}(T)$ shows a weak T dependence and is significantly suppressed compared to the mean-field line $B_{c2}(T)$ or the static "melting" (depinning) line. The results indicate that *intrinsic* quantum melting of the vortex lattice decoupled from the underlying pinning potential occurs well below B_{c2} at $T \to 0$.

DOI: 10.1103/PhysRevB.80.132503 PACS number(s): 74.25.Qt, 74.25.Dw, 74.78.Db

Melting of solids is one of the most fundamental physical phenomena that occur in nature. Of particular interest is a melting transition driven solely by quantum fluctuations (QFs).[1,2] Even at absolute zero, the solid can melt into liquid by changing some control parameters other than temperature T, such as pressure and magnetic field B. A well-known example is a solid to superfluid (quantum liquid) transition of ^{4}He induced by decreasing pressure. The $T=0$ transition, i.e., a quantum phase transition, has long been an active research area in condensed-matter physics and studied in various physical systems, which include the charge-density wave, Wigner crystals, quantum spin systems, ultracold atoms, and superconductors. In type-II superconductors, a vortex liquid state occupies a significant part of the phase diagram over broad T just below the upper critical field $B_{c2}(T)$. At high T, properties of vortex lines are dominated by thermal fluctuations, while at sufficiently low T, they are subject to QFs. If the QFs are large enough, the vortex solid may melt into a quantum vortex liquid (QVL),[1–3] as reported in several superconductors.[2,4–8] The experimental observation of quantum melting requires very low temperatures close to $T=0$ and high fields close to $B_{c2}(0)$. In the relevant T and B regions, however, the influence of the quenched disorder (pinning) inevitably contained in actual superconductors becomes nontrivial[9] and it results in a structural transition from an ordered lattice into a disordered solid. This accompanies a peak behavior in the critical current I_c vs B, known as a peak effect,[10] and it masks the observation of "intrinsic" quantum melting. In order to overcome this fact, the preparation of a sample with zero pinning is desirable, but it is actually difficult.

The influence of pinning is effectively reduced by driving vortices analogously to dynamic friction at a solid-solid interface. An important feature for a driven vortex lattice at a given velocity v is that the periodic lattice motion is disrupted due to combined influences of quenched disorder and thermal or quantum fluctuations and it disappears at a (dynamic) melting point.[11–13] A simple extrapolation of the melting points to the limit of $v \to \infty$ allows us to exclude the pinning effect and thus to determine the melting line in the limit of zero pinning. Employing this at low T, we can explore the *intrinsic* melting phenomenon in the quantum fluctuation regimes, but this was not attained in our preliminary work.[13]

Here, we report on dynamic melting of driven vortex lattice on amorphous (a-)Mo_xGe_{1-x} films detected by mode-locking (ML) experiments. From the systematic measurements of ML for different frequencies (velocities v of driven vortices at ML), currents (dissipation), T, and B, we determine the dynamic melting line $B^{\infty}_{c,dyn}(T)$ at $v \to \infty$ in nearly the whole B-T phase diagram. At low T, $B^{\infty}_{c,dyn}(T)$ shows a weak T dependence, deviating downward from the mean-field line $B_{c2}(T)$ or the static "melting" (depinning) line $B_c(T)$, which is determined by ordinary transport measurements. The results indicate that *intrinsic* quantum melting of the vortex lattice decoupled from the underlying pinning potential occurs at $\sim 0.8B_{c2}$, which is well below B_{c2}, in the limit $T \to 0$.

We prepared two 330-nm-thick a-Mo_xGe_{1-x} films with nearly the same superconducting properties by rf sputtering.[11] The one film (film 1) was attached to the cold plate of our ^{3}He-^{4}He dilution refrigerator and ML measurements were performed below 3.1 K. The other film (film 2) was directly immersed into liquid ^{4}He and measured at 4 K. The mean-field transition temperatures T_{c0} defined by a 95% criterion of the (normal-state) dc linear resistivity,[7] $\rho(T_{c0}) = 0.95\rho_n$, are 6.1 and 5.9 K and the zero-resistivity temperatures T_c are 6.0 and 5.8 K for films 1 and 2, respectively. In measuring the ML resonance, the ac current I_{rf} with a frequency f_{rf} up to 10 MHz was applied through an rf transformer. The field was applied perpendicular to the film surface.

We measure current-voltage (I-V) characteristics for film 1 in various B at fixed T ranging from 0.08 to 5.0 K. The critical current I_c is defined as a threshold current at which the vortices start to move and extracted from the I-V curves using a 10^{-7} V criterion.[12,14] The peak in $I_c(B)$ indicative of the peak effect is visible over the whole T region. As representatively shown in insets of Figs. 1(a) and 1(b), respectively, at 2.2 and 1.0 K, $I_c(B)$ takes a peak at $B_p = 7.7$ and 9.3 T before $I_c(B)$ vanishes at $B_c = 9.2$ and 11.1 T, where B_c nearly coincides with a characteristic field at which ρ falls to zero. Quite recently, we have found from measurements of flow noise that the peak field B_p in $I_c(B)$ marks the order-

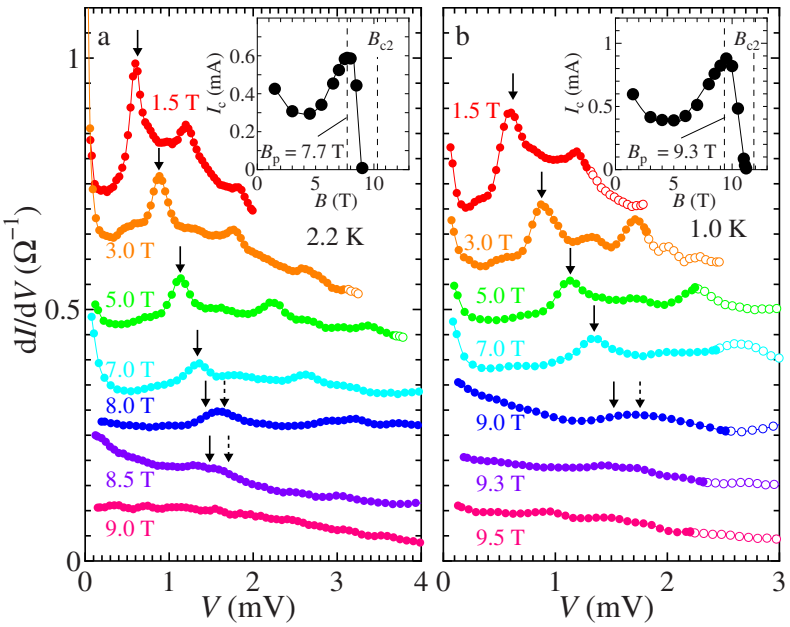

FIG. 1. (Color online) dI/dV vs V for film 1 taken at (a) 2.2 K and (b) 1.0 K for different B with superimposed 10 MHz I_{rf}. Location of the fundamental voltage steps calculated assuming a triangular vortex array moving in the perpendicular and parallel directions are indicated with full and dotted arrows, respectively. Full and open circles correspond to the data for which $\Delta T<0.01$ K and $\Delta T>0.01$ K, respectively. Inset: $I_c(B)$ at (a) 2.2 K and (b) 1.0 K. Vertical dashed lines indicate B_p (left) and B_{c2} (right) and other lines are guides for the eyes.

disorder transition (ODT) (Ref. 15) in the equilibrium solid phase from the weakly disordered vortex lattice [ordered phase (OP)] to highly disordered amorphouslike phase (DP).[14]

Now we briefly summarize the ML technique. When an object (vortex matter in this study) moves with velocity v in a periodic potential with a period a in the presence of combined dc and ac forces, steplike structure analogous to Shapiro steps found in Josephson junctions appears in the I-V characteristics.[16–21] The steps appear when the internal frequency $f_{int}=v/a$ of the system locks to the external frequency f_{rf} of the ac drive, more precisely, when the relation $qf_{int}=pf_{rf}$ is satisfied, where p and q are the integers. This phenomenon called the ML resonance has been observed not only in superconductors with periodic pinning[18,19] but also in those with *random* pinning,[16,20,21] such as amorphous films studied here, where a periodicity can be induced dynamically as a result of the coherent motion[22,23] of a vortex lattice. On approaching B_{c2} by increasing B at fixed T, there appears a critical field $B_{c,dyn}$ above which the moving vortices no longer exhibit dynamic ordering. This field $B_{c,dyn}$ is identified with a dynamic melting point.

At all $T(\geq 0.8$ K) measured, over the broad B in the solid phase including the peak-effect regime, we observe steplike structures indicative of ML in the I-V characteristics in the presence of superimposed ac drive I_{rf} with various amplitudes. To see the location of the ML steps clearly, we plot the differential conductance dI/dV against V. The main panel of Fig. 1(a) shows dI/dV vs V curves taken at 2.2 K for different B with superimposed 10 MHz I_{rf}. For each B, we select the data measured with $I_{rf}(=0.3-0.5$ mA) at which the width $\Delta I(I_{rf})$ of the ML current step takes a maximum. The peaks in the dI/dV vs V curves (i.e., ML steps) are clearly seen in B up to 8.0 T, which is larger than $B_p=7.7$ T, while they become less pronounced at higher B. Assuming a triangular vortex array moving in the direction perpendicular to one side of the triangle(s), we can calculate a value of the fundamental voltage step for a given $B(=1.5-7.0$ T), which satisfies the subharmonic resonant condition, as $lf_{rf}(\sqrt{3}\Phi_0 B/2)^{1/2}$, where l is the distance between the voltage contacts and Φ_0 the flux quantum,[24] and this is illustrated with a full arrow. The experimental data (i.e., the peak position) well coincides with the calculation. For 8.0 T($\approx B_p$), the data are better explained by a triangular vortex array moving in the *parallel* direction (a dotted arrow) or the mixture of the triangular arrays with both orientations, consistent with recent work that reveals the orientation change of the moving lattice around B_p.[24] Thus, the peaks in the dI/dV vs V curves shown in Fig. 1(a) indeed correspond to ML of driven vortex lattice.

A sign of ML persists up to 8.5 T, where the resonant peak becomes very board. At 9.0 T, all evidences for ML disappear, indicating the dynamic melting of the driven lattice. This characteristic is better displayed by plotting the step width ΔI against field, as shown in the inset of Fig. 2. Here, ΔI is obtained by integrating the peak of the dI/dV vs V curves with respect to the flux-flow baseline[21] as schematically illustrated in the inset (only the selected data are shown for clarity). After the slow decrease of ΔI with field, it drops rapidly and vanishes at high fields. This indicates the sudden collapse of the lattice order in motion, evidencing the dynamic melting into a moving liquid. We define the dynamic melting field $B_{c,dyn}$ as a field where $\Delta I(B)$ extrapolates linearly to zero (see a solid line). We find that at 2.2 K and higher T, the dynamic melting field $B_{c,dyn}$ is close to or slightly larger than B_c.

ML is observed down to the lowest temperatures studied, $T=0.8$ and 1.0 K, which correspond to $T/T_{c0}=0.13$ and 0.16, respectively. We representatively show in the main panel of

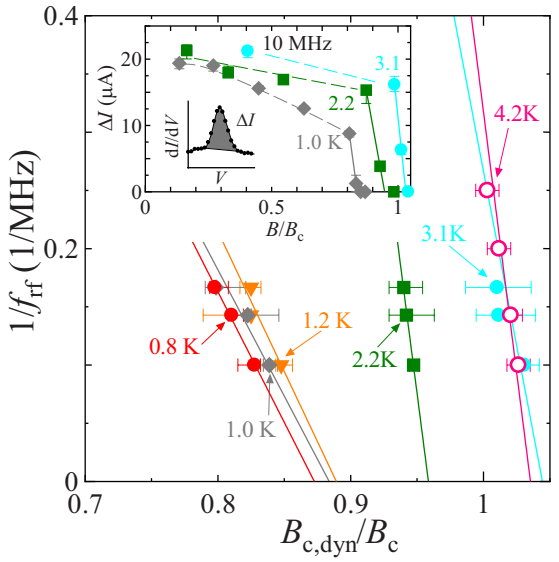

FIG. 2. (Color online) $B_{c,dyn}/B_c$ vs $1/f_{rf}$ at 0.8–3.1 K (full symbols) for film 1 and at 4.2 K (open circles) for the film studied in Ref. 11. Inset: ΔI vs B/B_c for selected data measured at 10 MHz I_{rf}, where the symbols correspond to those in the main panel. ΔI is obtained by integrating the peak of the dI/dV vs V curves with respect to the flux-flow baseline (see the inset). Full lines indicate the linear fits of the data and dashed lines are guide for the eyes.

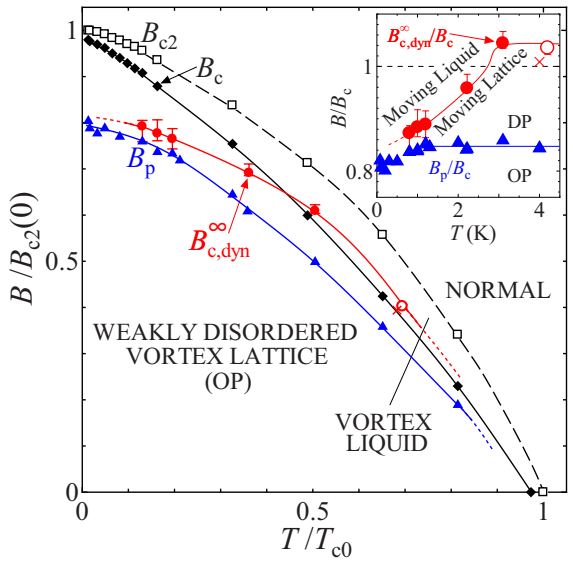

FIG. 3. (Color online) T dependences of $B^{\infty}_{c,dyn}$ (full circles), B_p (full triangles), B_c (full diamonds), and B_{c2} (open squares) for film 1. B and T axes are normalized by B_{c2} at $T=0$ and T_{c0}, respectively. An open circle and a cross, respectively, correspond to $B^{\infty}_{c,dyn}$ obtained in Ref. 11 and $B_{c,dyn}$ at 10 MHz for film 2. Inset: T dependences of $B_p(T)/B_c(T)$ and $B^{\infty}_{c,dyn}(T)/B_c(T)$, where the symbols correspond to those in the main panel. The B_p/B_c vs T and horizontal dashed lines mark the ODT and static melting (or depinning) transition, respectively, and the $B^{\infty}_{c,dyn}/B_c$ vs T line represents dynamic melting. All the lines are guides for the eyes.

Fig. 1(b) the dI/dV-V curves taken at 1.0 K for different B with superimposed 10 MHz I_{rf}(=0.2–0.3 mA). The ML peaks are clearly visible up to 7.0 T, where full arrows indicate the perpendicular lattice orientation, while they disappear at 9.0 or 9.3 T. Therefore, at 1.0 K, $B_{c,dyn}$ turns out to be around 9.3 T, which is close to B_p(=9.3 T) but clearly smaller than B_c(=11.1 T). This result is in contrast to what has been observed at higher T, where $B_{c,dyn}$ is close to B_c. Here we only present the data of ML measured at $T \geq 0.8$ K, considering possible heating effects due to the vortex motion. To examine the maximum power we can use for the ML measurements, we estimate the rise in the local temperature ΔT within the film as a function of T by measuring the T-dependent ρ in the normal state under 13 T with different I (i.e., different dissipation levels). We find that for some I-V data taken at 0.8 and 1.0 K, the power dissipated within the sample is not negligibly small at the second or third ML step. We confirm, however, that at any T studied, the heating effects do not seriously increase the local temperature at least up to the first ML step. Full and open circles in the main panels of Fig. 1 represent the data for which ΔT are below and above 0.01 K, respectively.

The values of $B_{c,dyn}$ presented above are obtained based on the data taken at a finite f_{rf}(=10 MHz). In order to estimate $B_{c,dyn}$ in the limit of the infinite vortex velocity ($v \rightarrow \infty$), namely, in the limit of zero pinning, we measure $B_{c,dyn}$ at different f_{rf}. In the main panel of Fig. 2, we plot with full symbols the reduced dynamic melting field $B_{c,dyn}/B_c$ [$B_{c,dyn}(T)$ divided by $B_c(T)$] against $1/f_{rf}$ at different T. Open circles (4.2 K) correspond to the data for a similar a-Mo_xGe_{1-x} film with T_c=6.1 K studied in Ref. 11. From a simple linear extrapolation of the data to $f_{rf}^{-1} \rightarrow 0$, we obtain the asymptotic value of $B_{c,dyn}(\equiv B^{\infty}_{c,dyn})$ at $f_{rf} \rightarrow \infty$ (i.e., $v \rightarrow \infty$).

The inset of Fig. 3 illustrates the T dependences of $B_p(T)$ (full triangles) and $B^{\infty}_{c,dyn}(T)$ (full circles) normalized by $B_c(T)$; i.e., the phase diagram near $B_c(T)$. An open circle and a cross, respectively, correspond to $B^{\infty}_{c,dyn}$ obtained in Ref. 11 and $B_{c,dyn}$ at 10 MHz for film 2. It is seen that $B_p(T)/B_c(T)$ is nearly independent of T except in the vicinity of $T=0$, indicating that the shapes of the $B_p(T)$ and $B_c(T)$ curves are similar to each other. A B_p/B_c vs T line marks ODT, a horizontal dashed line reflects the static melting or depinning line, and a $B^{\infty}_{c,dyn}/B_c$ vs T line represents dynamic melting. $B^{\infty}_{c,dyn}(T)$ is close to or slightly larger than $B_c(T)$ at high T, but upon cooling, it shows a decrease below about 2.5 K and seems to approach $B_p(T)$ at $T \rightarrow 0$. We display the dynamic melting line [$B^{\infty}_{c,dyn}(T)$] in the equilibrium $B-T$ phase diagram (see the main panel of Fig. 3), where the symbols correspond to those in the inset and the B and T axes are normalized by B_{c2} at $T=0$ and T_{c0}, respectively. An open circle and cross at $\sim$4 K ($T/T_{c0} \sim 0.7$) are plotted based on the ratio of $B^{\infty}_{c,dyn}/B_c$ (or $B_{c,dyn}/B_c$) because the exact values of $B_{c2}(0)$ are not obtained experimentally. One can see again that $B^{\infty}_{c,dyn}(T) \approx B_c(T)$ at high T ($>0.4T_{c0}$), while, on cooling below about $T=0.3T_{c0}$, the T dependence of $B^{\infty}_{c,dyn}(T)$ becomes very weak and $B^{\infty}_{c,dyn}(T)$ deviates downward from $B_c(T)$ and $B_{c2}(T)$, extrapolating to a field ($\approx 0.82B_{c2}$) far below B_{c2} in the limit $T \rightarrow 0$.

Considering the phenomenon from the frame of reference moving with the velocity v of driven vortex matter at ML, we may interpret the present results as follows. At ML, the vortices are localized, oscillating around their "equilibrium" positions.[20] Thus, $B_{c,dyn}(T)$ represents melting driven by ther-

mal or quantum fluctuations, in addition to shaking due to random pinning. In the limit $f_{rf} \rightarrow \infty$, the shaking effects become diminishingly small and $B^{\infty}_{c,dyn}(T)$ reflects melting for the vortex lattice that are decoupled from the underlying pinning potential.[11,23] Thus, we identify $B^{\infty}_{c,dyn}(T)$ as the intrinsic melting field. At low T, this intrinsic melting field is significantly suppressed compared to the static melting or depinning field $B_c(T)$, which is determined by ordinary transport measurements (ρ or I_c) in the presence of pinning[25] and approaches ODT $[B_p(0)]$ in the equilibrium solid phase. In the particular field region $B^{\infty}_{c,dyn} < B < B_c$, which corresponds to the equilibrium solid phase [amorphouslike DP (Ref. 14)], driven vortex matter does not form a moving lattice but dynamically melts into a moving liquid. This phenomenon occurs only at low T. Moreover, the T dependence of $B^{\infty}_{c,dyn}$ is much weaker than $B_c(T)$ in the low- $T(<0.3T_{c0})$ region. We propose from these results that quantum effects may play an important role in the vortex dynamics in the low-T and high-B regions, preventing the driven vortex solid from being dynamically ordered.

Now we compare the present result to the theory for quantum melting in the absence of quenched disorder (pinning effects) proposed by Blatter and co-workers.[2] Based on the Lindemann criterion, they argued that for thick films, the tilt modes of the vortex lattice is relevant for quantum melting, which is driven by Gaussian fluctuations. Considering the short-wavelength contributions, they calculate the quantum-melting field close to B_{c2} as

$$B^{G}_{m} = B_{c2}[1 - (2/\pi)\exp\{-(\pi^3 c_L^2/2)(R_Q/R_{eff})\} \times \exp\{(2/\sqrt{\pi}\nu)(2\pi/3 - 1/\sqrt{\pi}\nu)\}].$$

Here, c_L is the Lindemann number, $R_Q = h/(2\pi e^2) = 4.1\ \mathrm{k}\Omega$ (h is the Planck constant and e an elementary charge) is the quantum resistance, and R_{eff} is the effective sheet resistance, which is expressed as $\rho_n \nu/(\sqrt{2\pi}\xi)$ with a numerical constant ν of order unity and the coherence length ξ. Using material parameters of $\rho_n = 1.8\ \mu\Omega\mathrm{m}$ and $B_{c2}(0) = 12.7$ T for the present a-Mo_xGe_{1-x} film and choosing theoretical values of $c_L = 0.15$ and $\nu = 6$ of reasonable magnitude,[2] we can reproduce the intrinsic melting line $B^{\infty}_{c,dyn}(T)$ at $T \rightarrow 0$ by Eq. (1), where $B^{G}_{m}(0) = 0.82 B_{c2}(0)$. Suppression of the melting field near $T=0$ by reducing the pinning strength has been suggested by the microscopic theory of Ikeda, independent of the Lindemann approach.[3]

In conclusion, we observe intrinsic melting of a driven vortex lattice decoupled from the pinning potential down to near $T=0$ by ML and determine the intrinsic (dynamic) melting line $B^{\infty}_{c,dyn}(T)$ in nearly the entire B-T phase diagram. At low T, $B^{\infty}_{c,dyn}(T)$ is significantly suppressed compared to $B_{c2}(T)$ or the static melting line, indicating that intrinsic quantum melting occurs well below B_{c2} at $T \rightarrow 0$. We believe that this work will stimulate detailed research into the quantum-melting phenomenon and vortex states near $T=0$, which are important for understanding the nature of the $T=0$ insulating QVL phase just above the superconductor-insulator transition in thin superconducting films[1,26] and the quantum criticality in unconventional superconductors.[6]

[1] M. P. A. Fisher, Phys. Rev. Lett. **65**, 923 (1990).
[2] G. Blatter, B. Ivlev, Y. Kagan, M. Theunissen, Y. Volokitin, and P. Kes, Phys. Rev. B **50**, 13013 (1994).
[3] R. Ikeda, Int. J. Mod. Phys. B **10**, 601 (1996); K. Myojin, R. Ikeda, and S. Koikegami, Phys. Rev. B **78**, 014508 (2008).
[4] J. A. Chervenak and J. M. Valles, Jr., Phys. Rev. B **54**, R15649 (1996).
[5] M. M. Mola, S. Hill, J. S. Brooks, and J. S. Qualls, Phys. Rev. Lett. **86**, 2130 (2001).
[6] T. Shibauchi, L. Krusin-Elbaum, G. Blatter, and C. H. Mielke, Phys. Rev. B **67**, 064514 (2003).
[7] S. Okuma, Y. Imamoto, and M. Morita, Phys. Rev. Lett. **86**, 3136 (2001).
[8] S. Okuma, S. Togo, and M. Morita, Phys. Rev. Lett. **91**, 067001 (2003).
[9] A. D. Thakur, T. V. Chandrasekhar Rao, S. Uji, T. Terashima, M. J. Higgins, S. Ramakrishnan, and A. K. Grover, J. Phys. Soc. Jpn. **75**, 074718 (2006).
[10] P. H. Kes and C. C. Tsuei, Phys. Rev. B **28**, 5126 (1983).
[11] N. Kokubo, T. Asada, K. Kadowaki, K. Takita, T. G. Sorop, and P. H. Kes, Phys. Rev. B **75**, 184512 (2007).
[12] S. Okuma, J. Inoue, and N. Kokubo, Phys. Rev. B **76**, 172503 (2007); Int. J. Mod. Phys. B **21**, 3379 (2007).
[13] S. Okuma, H. Imaizumi, K. Suzuki, Y. Suzuki, and N. Kokubo, *Proceedings of the 25th International Conference on Low Temperature Physics, Amsterdam, 2008* [J. Phys.: Conf. Ser. **150**, 052200 (2009)]; S. Okuma, H. Imaizumi, Y. Suzuki, and N. Kokubo, *Proceedings of the 20th International Symposium on Superconductivity, Tsukuba, 2008* [Physica C **469**, 1063 (2009)].
[14] S. Okuma, K. Kashiro, Y. Suzuki, and N. Kokubo, Phys. Rev. B **77**, 212505 (2008).
[15] Y. Paltiel, E. Zeldov, Y. Myasoedov, M. L. Rappaport, G. Jung, S. Bhattacharya, M. J. Higgins, Z. L. Xiao, E. Y. Andrei, P. L. Gammel, and D. J. Bishop, Phys. Rev. Lett. **85**, 3712 (2000).
[16] A. T. Fiory, Phys. Rev. Lett. **27**, 501 (1971).
[17] M. J. Higgins, A. A. Middleton, and S. Bhattacharya, Phys. Rev. Lett. **70**, 3784 (1993).
[18] L. Van Look, E. Rosseel, M. J. Van Bael, K. Temst, V. V. Moshchalkov, and Y. Bruynseraede, Phys. Rev. B **60**, R6998 (1999).
[19] C. Reichhardt, R. T. Scalettar, G. T. Zimányi, and N. Grønbech-Jensen, Phys. Rev. B **61**, R11914 (2000).
[20] A. B. Kolton, D. Dominguez, and N. Grønbech-Jensen, Phys. Rev. Lett. **86**, 4112 (2001).
[21] N. Kokubo, K. Kadowaki, and K. Takita, Phys. Rev. Lett. **95**, 177005 (2005).
[22] Y. Togawa, R. Abiru, K. Iwaya, H. Kitano, and A. Maeda, Phys. Rev. Lett. **85**, 3716 (2000).
[23] A. E. Koshelev and V. M. Vinokur, Phys. Rev. Lett. **73**, 3580 (1994).
[24] N. Kokubo, B. Shinozaki, and P. H. Kes, Physica C **468**, 581 (2008).
[25] S. Okuma, K. Suzuki, and M. Kohara, Int. J. Mod. Phys. B **21**, 3371 (2007).
[26] V. M. Vinokur, T. I. Baturina, M. V. Fistul, A. Y. Mironov, M. R. Baklanov, and C. Strunk, Nature (London) **452**, 613 (2008).